

# QUASAR: A Universal Autonomous System for Atomistic Simulation and a Benchmark of Its Capabilities

Fengxu Yang<sup>1</sup> and Jack D. Evans<sup>\*1</sup>

<sup>1</sup>School of Physics, Chemistry and Earth Sciences, Adelaide University, North Terrace, Adelaide, 5005, South Australia, Australia

February 3, 2026

## Abstract

The integration of large language models (LLMs) into materials science offers a transformative opportunity to streamline computational workflows, yet current agentic systems remain constrained by rigid tool-calling approaches and narrowly scoped agents. In this work, we introduce QUASAR, a universal autonomous system for atomistic simulation designed to facilitate production-grade scientific discovery. QUASAR autonomously orchestrates complex multi-scale workflows across diverse methods, including density functional theory, machine learning potentials, molecular dynamics, and Monte Carlo simulations. The system incorporates robust mechanisms for adaptive planning, context-efficient memory management, and hybrid knowledge retrieval to navigate real-world research scenarios without human intervention. We benchmark QUASAR against a series of three-tiered tasks, progressing from routine tasks to frontier research challenges such as photocatalyst screening and novel material assessment. These results suggest that QUASAR can function as a general atomistic reasoning system rather than a task-specific automation framework. They also provide initial evidence supporting the potential deployment of agentic AI as a component of computational chemistry research workflows, while identifying areas requiring further development.

## 1 Introduction

The rapid advancement of agentic capabilities in large language models (LLMs) presents a compelling opportunity to transform computational chemistry for materials science research [1]. As a discipline fundamentally driven by complex computer-mediated workflows, computational chemistry tasks are naturally suited for integration with LLM-based automation, which can streamline tasks such as simulation setup, data interpretation, and error handling. This approach reduces both cognitive load and the technical burden associated with specialized software stacks and continuous human oversight. More importantly, it can serve as a low-risk, high-fidelity testing ground for systems that manage self-driving labs [2, 3].

Recent research demonstrates the effective integration of LLMs across multiple stages of computational chemistry pipelines. For example, Wang et al. developed DREAMS, a hierarchical multi-agent framework for density functional theory (DFT) materials simulations that combines a central LLM planner with domain-specific agents for atomistic structure generation, systematic convergence testing, HPC scheduling, and error handling [4]. Similarly, Zou et al.

---

\*Corresponding author: j.evans@adelaide.edu.au

introduced El Agente Q that dynamically generates, executes, and debugs quantum chemistry workflows from natural language prompts, integrating tools like RDKit, xTB, and ORCA for tasks such as geometry optimization and property prediction [5]. Additionally, Vriza et al. presented a framework for end-to-end atomistic simulations, using LLMs and specialized agents to automate processes from structure generation via Atomsk and interatomic potential discovery, to MD execution with LAMMPS and analysis using OVITO and Phonopy [6]. Several other frameworks have explored similar methods, highlighting the rapidly expanding ecosystem of intelligent, tool-augmented simulation platforms [7, 8, 9, 10].

Yet, most computational chemistry agentic systems remain constrained by rigid tool-calling paradigms and overly fine-grained agent role decompositions, which force models to operate within narrowly predefined functions and workflows. These design choices inherently limit the capacity of LLMs to navigate complex scenarios and engage in self-correction, effectively reducing reasoning engines to mere instruction followers. As a result, these systems struggle with tasks outside the curated demonstrations. Moreover, the extensive implementation of domain-specific tool calls introduces contextual overhead. These highly specialized agents increase system complexity and can lead to fragile operations, particularly in basic routing, coordination, and control logic. Together, these factors impose substantial engineering burdens, requiring careful manual design, continuous maintenance, and extensive human effort to stabilize and streamline agent workflows. This complexity ultimately undermines scalability, reliability, and adaptability, impeding the deployment of agentic systems in real-world computational chemistry settings.

In this work, we introduce QUASAR, a production-level universal atomistic computation system designed to overcome these limitations (Table 1). By combining a robust and modular architecture with simulation-optimized mechanisms, QUASAR enables seamless coordination across diverse computational workflows, ranging from quantum mechanical calculations to classical molecular simulations. Unlike conventional systems, which often require extensive manual setup or specialized expertise, QUASAR leverages the knowledge representation and reasoning capabilities of LLMs to automate complex decision-making processes, such as selecting optimal simulation parameters and dynamically adjusting computational strategies. This integration not only enhances usability, allowing researchers to interact with atomistic simulations more intuitively, but also improves flexibility, supporting a wide range of simulation tools and research objectives. By orchestrating LLM-driven reasoning with high-performance computational routines, QUASAR empowers autonomous scientific research, enabling rapid hypothesis testing, efficient exploration of chemical space, and reliable generation of predictive insights that are traditionally time- and expertise-intensive.

Table 1: Comparison of QUASAR with recent agentic computational chemistry systems. SE denotes semi-empirical methods.

Category	QUASAR	El Agente [5]	DREAMS [4]	LAMMPS-Agents [6]
Domain	DFT, MD, MC, MLP	DFT, SE	DFT	MD, MLP
Extensibility	Prompt-based	Code-based	Code-based	Code-based
Scope	Real-world Research	Textbook demonstrations	Textbook demonstrations	Textbook demonstrations
Deployment	Native Docker; Platform-agnostic	Closed Source; Commercial Cloud	Manual setup; Specific HPC only	Native Docker; Specific HPC only

## 2 System Architecture and Methods

As shown in Figure 1, QUASAR employs a three-agent architecture built upon LangChain [11]. The Strategist interprets user-defined research objectives and decomposes them into scientifically grounded subtasks; the Operator executes these subtasks by interfacing with atomistic simulation software, the local file system, and external resources, handling input preparation, job execution, and analysis; and the Evaluator assesses task completion, returning unsatisfactory results to the Operator for autonomous refinement.

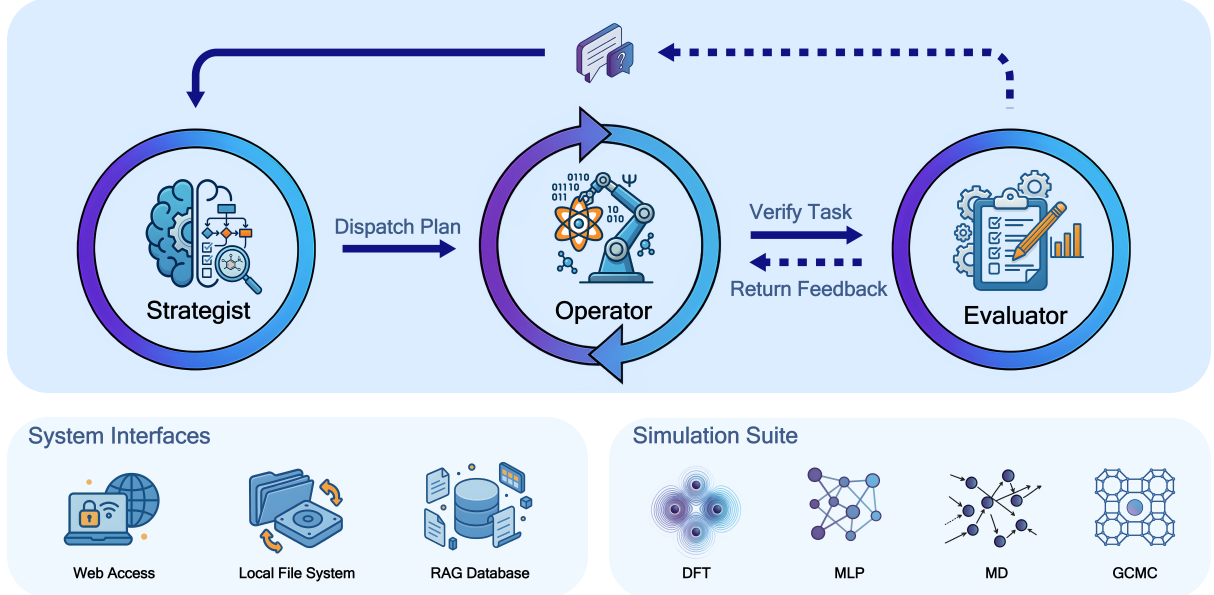


Figure 1: Overview of the QUASAR architecture, where dashed lines represent optional feedback paths for iterative refinement.

The software stack currently included in QUASAR bridges multiple levels of theory using only open-source software. This includes Quantum ESPRESSO [12] for ab initio DFT calculations, MACE [13] for machine-learned potentials (MLP), LAMMPS [14] for classical molecular dynamics (MD), and RASPA3 [15] for grand canonical Monte Carlo (MC) simulations, unified through ASE [16] and pymatgen [17] for structure manipulation and analysis. The multiscale integration allows QUASAR to autonomously chain simulations across length and time scales. As one example, the system can parameterize force fields from quantum calculations and then deploy the resulting force field for large-scale dynamics or adsorption studies that would be intractable at the DFT level.

In addition to the predefined computational pillars, QUASAR is designed to support dynamic tool integration. As summarized in Table 1, many existing agentic systems rely on hard-coded agent hierarchies and tightly scoped domain-specific tools, which can make their architectures rigid and difficult to extend. Adding new tools to these systems often requires major architecture re-engineering, introducing new specialized agents and functions. QUASAR significantly lowers the barrier to extensibility. For immediate requirements, users can trigger tool installation directly via natural-language prompts. For stable, long-term solutions, developers can bundle tools into the Docker environment with minimal prompt updates. Both pathways significantly reduce integration costs and reinforce the flexibility-oriented design of QUASAR.

### 2.1 Robust and Adaptive Planning

Planning is the most critical stage of the system, as it explicitly defines the Operator’s scope of action and establishes the core principles guiding execution. For complex computational chem-

istry objectives, the direct plan from the Strategist may occasionally overlook key considerations or domain-specific cues. This plan can in turn lead the Operator toward suboptimal or inappropriate actions. For example, in a multi-stage free energy or adsorption workflow, a plan may omit prerequisite equilibration steps which can potentially lead to physically inconsistent or unreliable results. Therefore, to maintain high-quality plan generation, we adopted a double-pass planning mechanism: an initial plan produced by the Strategist is subjected to a second-pass review that explicitly checks missing elements before execution.

QUASAR also incorporates an iterative feedback loop with optional human-in-the-loop (HITL) integration to address scenarios where “one-shot” generation falls short of the scientific objective. After a completed run, researchers may either trigger an automated improvement cycle or provide specific insights. This prompts the Strategist to shift from a generative role to a diagnostic one, critically analyzing the previous outputs to propose targeted improvements or corrections.

To further align planning with diverse research objectives, the Strategist is regulated by two user-adjustable parameters: Granularity and Accuracy. Granularity controls task decomposition depth (number of tasks), determining how frequently evaluation and context compression occur. Finer granularity enables more frequent checkpoints but may introduce unnecessary fragmentation for straightforward tasks, while coarser granularity reduces overhead for simpler workflows. Accuracy balances computational cost against precision: “eco” mode employs computationally efficient methods for rapid screening, whereas “pro” mode applies rigorous approaches for high-accuracy results at the expense of increased computation time. These parameters enable QUASAR to dynamically adapt its planning and memory architecture to specific research needs. Straightforward tasks such as variable-cell (VC) relaxation in Quantum ESPRESSO benefit from low granularity settings, avoiding redundant task fragmentation and evaluations that would otherwise degrade execution efficiency. This flexibility allows researchers to optimize the balance between thoroughness and computational economy based on their specific objectives.

## 2.2 Context and Memory Efficiency

Tuning context is one of the major challenges in agentic design as it governs the quality and stability of agent orchestration [18]. Much like human collaboration, the clarity and volume of the information passed between agents directly dictate the effectiveness of the collective outcome. While recent LLMs feature significantly expanded context windows, they are not infinite. More importantly, analogous to human cognition, as the context length expands, the likelihood of losing focus on the previous conversation increases [19]. For instance, as the Operator progresses through a list of tasks, the accumulating context can become excessively large, effectively diluting the model’s understanding of completed tasks and escalating the API costs.

To mitigate this, our system optimizes context sharing at two levels: between individual tasks (task-task) and across distinct execution sessions (run-run). Once the Evaluator verifies the successful completion of a task, it condenses the task context by distilling the valuable actions and outcomes while discarding noise and failed attempts. This not only reduces the overall context length but also strengthens contextual coherence. To support the replanning mechanism discussed earlier, the system additionally maintains long-term memory across runs. In contrast to task-level compression, upon completion of a run the system saves a task-level summary produced by the Evaluator, together with a complete summary generated by the Operator at the final step, to the local filesystem in Markdown format. Enabling seamless connection to prior execution context, QUASAR provides an incremental workflow that drives continuous improvement, and also provides an accessible entry point for human review.

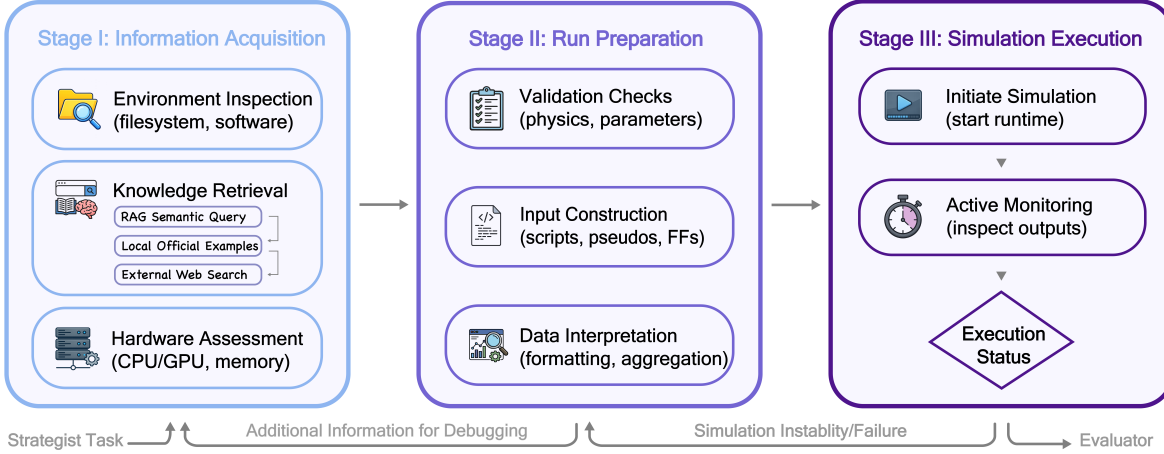


Figure 2: A three-stage pipeline illustrating how the Operator coordinates end-to-end simulation tasks.

### 2.3 Long Simulation Handling

The system is designed for reliable operation in real-world scenarios where interruptions from API exhaustion, wall-time limits, or unexpected shutdowns are common. To address this, we implemented persistent state management, ensuring that the full agent state (conversation history and completed steps) is automatically checkpointed after every execution. This allows the system to recover from interruptions without any loss of progress. In addition to the generic checkpointing, QUASAR is specifically optimized for recovering interrupted simulations. When an interrupted simulation is resumed, the system auto-injects an interruption-awareness prompt that guides the Operator to restart from the most recent intermediate state rather than restarting the workflow. For example, during a VC relaxation with Quantum ESPRESSO, the Operator agent will attempt to resume the calculation from the partially relaxed structure instead of initiating a fresh run, significantly reducing redundant computation.

The successful execution and completion of a simulation does not necessarily guarantee scientific correctness or numerical precision. For instance, in software like Quantum ESPRESSO, if a convergence threshold is set too strictly or the system is unstable, the program may reach its default maximum step limit (e.g., 100 steps) and exit without achieving convergence. While the job appears “Done” in the output, the simulation has not been completed. In long-duration or computationally expensive simulations, these “silent failures” lead to significant waste of time and resources. To address this, we introduce a check-in mechanism that allows users to configure the inspection frequency for the Operator (default: 15 minutes). At each check-in, the Operator evaluates intermediate outputs to assess whether the simulation is progressing correctly. If clear issues are detected, such as a lack of DFT convergence, the Operator terminates the run and attempts to reconstruct or optimize the input parameters or other related factors.

### 2.4 Hybrid Knowledge Retrieval

QUASAR employs a domain-specific Retrieval-Augmented Generation (RAG) database, indexing documentation and source code to mitigate hallucinations arising from limited or outdated LLM knowledge. However, simulation engines such as LAMMPS and Quantum ESPRESSO rely on highly specialized and unique input syntaxes. Their official example scripts and input files typically contain very minor natural language comments and instead rely on a separate overview README file for explanation. This sparse semantic context makes embedding-based retrieval challenging, as the technical syntax and domain-specific parameters lack the descriptive text that vector search relies upon. To overcome this limitation, QUASAR exposes a local repository

of example input files directly to the Operator. Rather than relying solely on semantic embeddings, the Operator leverages its reasoning capabilities to navigate to the provided directories, interpret filenames, and parse README files to identify relevant reference examples.

Additionally, QUASAR implements a hierarchical knowledge-access protocol via the Operator’s system prompt to further enhance the retrieval efficiency. When the Operator has high confidence in the required simulation physics and input syntax, it proceeds autonomously using its internal knowledge. If uncertainty arises, it is guided to first perform semantic similarity matching via RAG to relevant documentation or code examples. When a RAG query is insufficient or ambiguous, the system uses the logical inference approach, in which the Operator systematically explores the provided example repositories and infers appropriate simulation patterns. Only as a final fallback does the Operator expand its search space to external web resources. By escalating from quick-access internal data to resource-heavy external searches only when necessary, QUASAR allows the system to reliably support complex simulation setups and debugging tasks, ensuring higher rates of successful simulation execution while reducing unnecessary action overhead.

## 2.5 Containerized Environment and HPC Optimization

Usability and security are two critical considerations in the design of QUASAR. To ensure seamless deployment across diverse environments, QUASAR provides cross-platform Docker containers pre-packaged with the suite of computational tools stated previously. This includes specialized images optimized for CUDA and ROCm to facilitate hardware-accelerated inference (e.g., for MACE models). Moreover, from a security perspective, the containerized nature inherently prevents catastrophic actions such as deletion of system files. QUASAR can also operate completely offline and supports integration with locally hosted open-source LLMs, ensuring that sensitive or confidential data remains secure.

QUASAR is deeply optimized for high-performance computing (HPC), and its Docker containers are designed to run natively under Singularity/Apptainer on HPC systems. Its non-interactive execution mode paired with a built-in restart mechanism, allows entire workflows to be submitted and reliably executed as standard batch jobs. The system currently does not support agent-driven HPC job submission, as it is designed to prioritize broad compatibility across diverse computational environments. The variations in HPC schedulers, configurations, and site-specific policies make it difficult to reliably abstract them into a single generalized interface. Therefore, for specialized deployments targeting a single fixed HPC environment, additional facility-specific submission tooling could be incorporated, but this falls outside the current design scope of QUASAR.

## 2.6 User Interfaces

To connect the system backend with end users, QUASAR provides a Command Line Interface (CLI) with essential control and monitoring capabilities. The CLI permits real-time tracking of agent progress and provides granular visibility into execution details, including the generated plan and code snippets. It also supports a robust restart mechanism, allowing users to resume execution after interruptions. For advanced use cases, an optional web-based graphical user interface (GUI) is available through licensing agreements, offering streamlined monitoring, fine-grained execution control, and visualization.

## 3 Results

We evaluated QUASAR using a three-tiered benchmark suite (Table 2) with the `gemini-3-flash-preview` LLM. All tiers were executed in “pro” accuracy mode without human interventions, with

Tier I configured for “low” granularity and Tiers II and III for “high” granularity. Detailed metadata, including hardware details and token usage, is provided in the Supporting Information.

Table 2: Overview of the three-tiered benchmarking suite used to validate QUASAR. Row headers are highlighted in grey to distinguish tiers.

Test Case	Prompt	Result
<i>Tier I: Task Execution</i>		
<b>K-point Convergence</b>	Calculate the k-point density to converge bulk Cu energy to 1 meV/atom.	$\Delta E < 0.6$ meV True
<b>NPT Equilibration</b>	Calculate the density of water at 298 K and 1 bar.	$\bar{\rho} = 0.99786$ g/cm <sup>3</sup> Ref: 0.99709 g/cm <sup>3</sup> [20]
<b>Helium Void Fraction</b>	Calculate the helium-accessible void fraction and pore volume for IRMOF-1.cif at 298 K.	$\phi_{He} = 0.7988$ Ref: approx. 0.80 [21]
<i>Tier II: Workflow Orchestration</i>		
<b>Band Gap</b>	Calculate the electronic band gap for bulk nickel oxide.	Run 1: $E_g = 2.72$ eV Run 2: $E_g = 2.57$ eV Run 3: $E_g = 4.18$ eV Ref: 4.0 eV [22]
<b>Adsorption Isotherm</b>	Calculate the adsorption isotherm for CO <sub>2</sub> in UiO-66 at 298 K.	$n_{10 \text{ bar}} = 5.98$ mmol/g Ref: approx. 5 - 7 mmol/g [23]
<b>Melting Point</b>	Calculate the melting point of aluminum.	$T_m = 934.47 \pm 0.61$ K Ref: 933.45 K [20]
<i>Tier III: Frontier Research</i>		
<b>Photocatalyst Screening</b>	Determine which 5% La-doped ATaO <sub>3</sub> perovskite (A = Li, Na, K) exhibits the best photocatalytic degradation performance against methyl orange under UV irradiation.	NaTaO <sub>3</sub> : 5% La
<b>Gas Separation</b>	Determine which COF maximizes the Xe/Kr adsorption selectivity at 298 K. The experimental CIF structures are provided.	COF-X-Br
<b>Virtual MOF Assessment</b>	Determine the CO <sub>2</sub> adsorption performance and mechanical properties of the provided MOF.	Non-porous ( $q \approx 0$ ); Stiff ( $K = 165.8$ GPa)

### 3.1 Tier I. Task Execution

To verify the baseline usability of the system, we selected three simple representative tasks spanning distinct methodological archetypes. These foundational tests are designed to confirm that QUASAR can reliably execute well-defined, single-step calculations that form the building blocks of more complex workflows. While individually straightforward, each task requires correct parameter selection, appropriate software invocation, and accurate interpretation of outputs.

The first task involves DFT k-point convergence, which ensures reliable Brillouin-zone sampling for electronic structure simulations and is a prerequisite for any production-quality periodic calculation. The second task addresses *NPT* ensemble equilibration in molecular dynamics, which is essential for obtaining thermodynamically consistent densities before production simulations and validates the capacity of QUASAR to configure and monitor classical simulation

protocols. The third task focuses on helium void-fraction analysis, a Monte Carlo characterization method used to quantify accessible porosity in porous materials for gas storage and separation applications. Together, these three tasks span quantum mechanical, classical mechanics, and Monte Carlo methods, providing a representative cross-section of the computational toolkit commonly employed in materials science research.

### 3.2 Tier II. Workflow Orchestration

Moving beyond individual calculations, Tier II evaluates the ability of QUASAR to decompose high-level scientific questions into coherent, multi-step computational workflows.

The first task involves calculating the electronic band gap of bulk nickel oxide, which challenges the system to handle strongly correlated transition metal oxides. This requires optimizing the crystal structure, correctly initializing the Type-II antiferromagnetic ordering, and applying an appropriate Hubbard  $U$  correction (DFT+ $U$ ) or hybrid functional to accurately reproduce the band gap.

The second task focuses on generating CO<sub>2</sub> adsorption isotherms for UiO-66 at 298 K. To produce a full isotherm, the system must orchestrate a series of Grand Canonical Monte Carlo (GCMC) simulations, which involves selecting appropriate force fields, preparing the simulation cell, and systematically sweeping through a range of chemical potentials (pressures) to map the isotherm.

The final task in this tier requires determining the melting point of aluminum, testing the ability of QUASAR to characterize phase transitions using molecular dynamics methods. The agent must autonomously infer and correctly sequence all prerequisite computational steps, such as system equilibration and phase initialization prior to executing the melting-point calculation. It then needs to select a reliable approach such as the two-phase coexistence method or temperature curves to accurately reproduce the solid–liquid transition temperature.

### 3.3 Tier III. Frontier Research

While the Tier II tasks demonstrate strong potential for real-world applications, they are well-documented in the literature and possibly represented in LLM training data. Tier III therefore targets recent or open research problems that lack established protocols, thereby testing the ability of the system to reason and explore without bias.

We tasked QUASAR with screening 5% La-doped ATaO<sub>3</sub> perovskites (A = Li, Na, K) for the photocatalytic degradation of methyl orange under UV irradiation. This complex query requires the agent to compute and align band edges relative to relevant redox potentials, assess the impact of doping on the optical gap, and evaluate defect formation energies. This task is based on recent published work from our lab [24].

The system was further challenged to identify which candidate covalent organic framework (COF) maximizes selectivity for xenon over krypton (Xe/Kr) at 298 K, from a selection of two unpublished COF structures. Research currently under review features these structures and they were experimentally verified. This task demands a comparative screening workflow that captures subtle host–guest interactions distinguishing these two noble gases, necessitating precise force-field selection and competitive adsorption simulations.

Finally, we provided the system with a novel material structure generated via latent diffusion that is not yet experimentally synthesized [25]. We tasked the agent with simulating its mechanical properties and CO<sub>2</sub> adsorption capacity. This stress test evaluates robustness in handling potentially unstable or unoptimized geometries, requiring structural integrity validation (e.g., via elastic tensor calculations) before proceeding to functional property prediction.

## 4 Discussion

The performance of QUASAR in Tier I and Tier II highlighted both the strengths and limitations of reasoning-driven computation. The system achieved accurate results with efficiency and rigor across all cases in these tiers, except for the Tier II NiO band gap calculation. In that case, the system failed to obtain an accurate value for the first run and required two further auto-improvement run contexts to recognize the need to switch to the higher-fidelity Heyd–Scuseria–Ernzerhof (HSE) method. This behavior likely reflects the strong training priors of the LLM, as DFT+ $U$  is overwhelmingly reported as the default approach for NiO in the literature. However, with the auto-improvement mechanism, QUASAR was able to escape this “local optimum” and progress toward a more accurate solution, illustrating the value of iterative, incremental approaches to goal-directed computation and highlighting the role of HITL guidance (i.e. signaling an auto-improvement loop) in achieving robust results.

Building upon this foundation, it underscores the importance of Tier III testing, which evaluates not only the robustness of trained routines but also the capacity for LLM to apply its learned knowledge in novel scenarios. In this tier, the final photocatalyst screening results correctly recreated the published result [24], and the gas separation and virtual MOF cases are validated as physically reasonable and methodologically reliable (see Supporting Information). Importantly, the performance of QUASAR in Tier III challenges the conventional assumption that materials research requires HITL guidance. These tasks did not undergo auto-improvement and the system performed end-to-end screening, method selection, and analysis, suggesting that agentic AI systems can independently execute complex scientific workflows with minimal or no human intervention. Our results highlight that QUASAR, and similar systems, may exhibit a level of autonomy that approaches that of expert researchers, while the boundaries of this capability remain to be fully determined.

Ultimately, these findings indicate that QUASAR is not merely an automation layer over existing simulation tools, but a fundamentally different paradigm for conducting atomistic research. Rather than encoding fixed workflows or predefined procedural pipelines, QUASAR demonstrates reasoning-driven orchestration, where planning, execution, evaluation, and refinement emerge from coordinated agent cognition. This shift is critical: the system does not depend on hard-coded domain logic, but instead exhibits generalizable scientific competence across heterogeneous tasks, methods, and research contexts. The ability of a single architecture and control logic to operate effectively across all three tiers indicates that QUASAR appears to capture transferable structure in scientific problem-solving. This suggests that QUASAR exhibits flexibility across the tested task types, though generalization beyond the evaluated benchmark suite requires further investigation. The reliance of this system on LLM capabilities means performance is bounded by the underlying domain knowledge and in-context learning ability of the chosen model.

Additionally, QUASAR achieved correct and high-quality results across all three benchmark tiers using a lightweight model `gemini-3-flash-preview`. This suggests that frontier models, such as `gemini-3-pro-preview` with enhanced reasoning capabilities, may not only pass the proposed benchmarks but do so with greater efficiency and rigor. The API costs when using `gemini-3-flash-preview` are also cost-effective: approximately \$1 USD for Tier I (single-step) and \$10 USD for Tier II test cases. Although Tier III scenarios incur higher costs ranging from \$10 USD to \$30 USD, these remain manageable given the complexity of the tasks and the cost can be further reduced by employing context caching to avoid redundant token processing [26].

## 5 Summary and Outlook

In this work, we introduced QUASAR, an open-source, portable, and universal atomistic computation system designed to transition agentic AI from simple demonstrations and basic task

handling toward production-grade scientific discovery. The flexible architecture of QUASAR supports further customization with minimal effort, such as the seamless integration of additional tools.

Through our Tier III benchmarking, QUASAR demonstrates that LLMs, when properly orchestrated, are capable of executing sophisticated computational chemistry tasks with a level of scientific rigor comparable to that of human researchers. This work serves as a proof of concept that modern AI has the potential to automate the vast majority of standard computational workloads, freeing the scientific process from the bottlenecks of manual execution. This positions QUASAR as a prototype for human–AI collaborative workflows in computational chemistry, where AI handles routine orchestration while humans provide scientific direction, judgment on ambiguous cases, and validation of results.

Beyond the `gemini-3-flash-preview` evaluated in this study, a diverse array of frontier LLMs, along with specialized small-scale models tailored for computational chemistry tasks, continue to emerge [27]. Given this diversity, selecting the best-performance model remains challenging when relying solely on success rates. It is imperative that future directions focus on developing comprehensive benchmarks (beyond the limited set employed in this study) to evaluate not only whether scientific objectives are achieved, but also the broader capabilities underlying the success. These benchmarks are necessary to fairly test the strategies employed, and the efficiency of decision-making across different models and agentic systems.

Our study also offers a perspective on the necessary evolution of the current scientific process as AI capabilities are reaching unprecedented heights. As execution, debugging, and workflow construction become automated, the primary role of human researchers shifts toward conceptual framing and theoretical innovation. This transition does not displace scientists but reallocates cognitive responsibility, enabling human researchers to prioritize scientific scope and hypotheses. We envision that AI may fundamentally reshape the structure and dynamics of the research lifecycle in the near future.

## Supporting Information

All code and data for this research are available on Zenodo: [10.5281/zenodo.18409876](https://doi.org/10.5281/zenodo.18409876). Additionally, the source code is available on GitHub , and the docker images for QUASAR deployment are hosted on DockerHub .

## Acknowledgements

J.D.E. is the recipient of an Australian Research Council Discovery Early Career Award (project number DE220100163) funded by the Australian Government. The Phoenix HPC service at the Adelaide University is acknowledged for providing high-performance computing resources. This research was supported by the Australian Government’s National Collaborative Research Infrastructure Strategy (NCRIS), with access to computational resources provided by Pawsey Supercomputing Research Centre through the National Computational Merit Allocation Scheme. We thank Mohamad Moosavi (University of Toronto) and his team for thought-provoking discussion.

## References

- [1] Wei, J. *et al.* From AI for Science to Agentic Science: A Survey on Autonomous Scientific Discovery (2025). URL <http://arxiv.org/abs/2508.14111>. ArXiv:2508.14111.
- [2] Tom, G. *et al.* Self-Driving Laboratories for Chemistry and Materials Science. *Chemical Reviews* **124**, 9633–9732 (2024). URL <https://pubs.acs.org/doi/10.1021/acs.chemrev.4c00055>.

[3] Inizan, T. J. *et al.* System of Agentic AI for the Discovery of Metal-Organic Frameworks (2025). URL <http://arxiv.org/abs/2504.14110>. ArXiv:2504.14110.

[4] Wang, Z. *et al.* DREAMS: Density Functional Theory Based Research Engine for Agentic Materials Simulation (2025). URL <http://arxiv.org/abs/2507.14267>. ArXiv:2507.14267.

[5] Zou, Y. *et al.* El Agente: An autonomous agent for quantum chemistry. *Matter* **8**, 102263 (2025). URL <https://www.sciencedirect.com/science/article/pii/S2590238525003066>.

[6] Vriza, A., Kornu, U., Koneru, A., Chan, H. & Sankaranarayanan, S. K. R. S. Multi-agentic AI framework for end-to-end atomistic simulations. *Digital Discovery* **5**, 440–452 (2026). URL <https://pubs.rsc.org/en/content/articlelanding/2026/dd/d5dd00435g>.

[7] Pham, T. D., Tanikanti, A. & Keçeli, M. ChemGraph: An Agentic Framework for Computational Chemistry Workflows (2025). URL <http://arxiv.org/abs/2506.06363>. ArXiv:2506.06363.

[8] Ghafarollahi, A. & Buehler, M. J. Automating alloy design and discovery with physics-aware multimodal multiagent AI. *Proceedings of the National Academy of Sciences* **122**, e2414074122 (2025). URL <https://pnas.org/doi/10.1073/pnas.2414074122>.

[9] Mendible-Barreto, O. A. *et al.* DynaMate: leveraging AI-agents for customized research workflows. *Molecular Systems Design & Engineering* **10**, 585–598 (2025). URL <https://pubs.rsc.org/en/content/articlelanding/2025/me/d5me00062a>.

[10] Nduma, R., Park, H. & Walsh, A. Crystalyse: a multi-tool agent for materials design (2025). URL <http://arxiv.org/abs/2512.00977>. ArXiv:2512.00977.

[11] Chase, H. LangChain (2022). URL <https://github.com/langchain-ai/langchain>. Original-date: 2022-10-17T02:58:36Z.

[12] Giannozzi, P. *et al.* Advanced capabilities for materials modelling with Quantum ESPRESSO. *Journal of Physics: Condensed Matter* **29**, 465901 (2017). URL <https://iopscience.iop.org/article/10.1088/1361-648X/aa8f79>.

[13] Batatia, I., Kovács, D. P., Simm, G. N. C., Ortner, C. & Csányi, G. MACE: Higher Order Equivariant Message Passing Neural Networks for Fast and Accurate Force Fields (2023). URL <http://arxiv.org/abs/2206.07697>. ArXiv:2206.07697.

[14] Thompson, A. P. *et al.* LAMMPS - a flexible simulation tool for particle-based materials modeling at the atomic, meso, and continuum scales. *Computer Physics Communications* **271**, 108171 (2022). URL <https://www.sciencedirect.com/science/article/pii/S0010465521002836>.

[15] Ran, Y. A. *et al.* RASPA3: A Monte Carlo code for computing adsorption and diffusion in nanoporous materials and thermodynamics properties of fluids. *The Journal of Chemical Physics* **161**, 114106 (2024). URL <https://pubs.aip.org/jcp/article/161/11/114106/3312873/RASPA3-A-Monte-Carlo-code-for-computing-adsorption>.

[16] Hjorth Larsen, A. *et al.* The atomic simulation environment—a Python library for working with atoms. *Journal of Physics: Condensed Matter* **29**, 273002 (2017). URL <https://iopscience.iop.org/article/10.1088/1361-648X/aa680e>.

[17] Ong, S. P. *et al.* Python Materials Genomics (pymatgen): A robust, open-source python library for materials analysis. *Computational Materials Science* **68**, 314–319 (2013). URL <https://www.sciencedirect.com/science/article/pii/S0927025612006295>.

[18] Abou Ali, M., Dornaika, F. & Charafeddine, J. Agentic AI: a comprehensive survey of architectures, applications, and future directions. *Artificial Intelligence Review* **59**, 11 (2025). URL <https://doi.org/10.1007/s10462-025-11422-4>.

[19] Du, Y. *et al.* Christodoulopoulos, C., Chakraborty, T., Rose, C. & Peng, V. (eds) *Context Length Alone Hurts LLM Performance Despite Perfect Retrieval*. (eds Christodoulopoulos, C., Chakraborty, T., Rose, C. & Peng, V.) *Findings of the Association for Computational Linguistics: EMNLP 2025*, 23281–23298 (Association for Computational Linguistics, Suzhou, China, 2025). URL <https://aclanthology.org/2025.findings-emnlp.1264/>.

[20] Informatics, N. O. o. D. a. NIST Chemistry WebBook. URL <https://webbook.nist.gov/chemistry/>.

[21] RASPA manual 23 May 2021 – iRASPA. URL <https://iraspa.org/download/raspa-manual-23-may-2021/>.

[22] Hüfner, S. Electronic structure of NiO and related 3d-transition-metal compounds. *Advances in Physics* **43**, 183–356 (1994). URL <http://www.tandfonline.com/doi/abs/10.1080/00018739400101495>.

[23] Jajko, G., Kozyra, P., Gutiérrez-Sevillano, J. J., Makowski, W. & Calero, S. Carbon Dioxide Capture Enhanced by Pre-Adsorption of Water and Methanol in UiO-66. *Chemistry – A European Journal* **27**, 14653–14659 (2021). URL <https://chemistry-europe.onlinelibrary.wiley.com/doi/10.1002/chem.202102181>.

[24] Matthews, R. K. *et al.* La Doping ATaO<sub>3</sub> (A = Li, Na, K) to Improve Performance for Photocatalytic Pollutant Degradation. *Chemistry of Materials* **37**, 3696–3708 (2025). URL <https://pubs.acs.org/doi/10.1021/acs.chemmater.4c03443>.

[25] Simkus, V. *et al.* Mofasa: A Step Change in Metal-Organic Framework Generation (2025). URL <http://arxiv.org/abs/2512.01756>. ArXiv:2512.01756.

[26] Yan, J. *et al.* ContextCache: Context-Aware Semantic Cache for Multi-Turn Queries in Large Language Models (2025). URL <http://arxiv.org/abs/2506.22791>. ArXiv:2506.22791.

[27] Shi, Z. *et al.* MDAgent2: Large Language Model for Code Generation and Knowledge Q&A in Molecular Dynamics (2026). URL <http://arxiv.org/abs/2601.02075>. ArXiv:2601.02075.